

Buckling of Near-Perfect Steel Torispherical and Hemispherical Shells Subjected to External Pressure

J. Blachut,* G. D. Galletly,† and D. N. Moreton‡
University of Liverpool, Liverpool, England, United Kingdom

The aims of the present series of tests on externally pressurized machined steel domed ends were twofold. The first was to verify the recently predicted and unusual variation of a dome's buckling resistance with the knuckle radius-to-diameter (r/D) ratio. The second was to verify that optimizing a dome's geometry, while keeping the weight constant, can bring substantial increases in the buckling strength. The agreement between the experimental results and the theoretical predictions is very good. The initial increase in the buckling strength, its reversal, the minimum buckling strength, and the rapid increase thereafter, all as predicted by theory, are confirmed by tests. The tests on near-perfect shells highlight the sensitivity of the buckling strength of torispherical shells to the r/D ratio, in the range $0.4 < r/D < 0.5$. In the optimization study, in which the geometric ratios D/t , r/D , and R_s/D were varied, the ratio of the buckling strengths of the best and the worst shapes is more than 5:1. The best and worst shapes have the same weight; it is clear that optimizing a dome's shape can produce substantial increases in strength. The good agreement between the test results and theoretical predictions is further confirmation of the adequacy of the BOSOR 5 shell buckling program for problems of this type.

Nomenclature

D	= diameter of hemispherical/torispherical shell (see Fig. 1)
E	= modulus of elasticity
n	= number of waves in the circumferential direction
p_c	= buckling pressure obtained from BOSOR 5
p_{expt}	= experimental buckling strength
p_H	= bifurcation buckling pressure of reference hemisphere
p_T	= buckling/collapse pressure of equivalent torisphere
p_{yp}	= yield pressure of spherical shell ($4\sigma_{yp} t/D$)
r	= radius of knuckle in torisphere (see Fig. 1a)
R_s	= radius of spherical part in torispherical shell (see Fig. 1a)
s	= meridional arc length measured from apex (see Fig. 1a)
t	= thickness of torisphere
\bar{t}	= mean thickness of torisphere measured on eight meridians
t_o	= thickness of reference hemisphere
V_H	= volume enclosed by reference hemisphere
V_T	= volume enclosed by torisphere
ν	= Poisson's ratio
σ_{yp}	= yield point of material

Introduction

RECENT calculations on the buckling strength of externally pressurized perfect torispherical and hemispherical shells^{1,2} (see Fig. 1) lead to the curves shown in Fig. 2 (for $R_s/t = 300$). For $r/D < 0.35$, the buckling pressures increase with an increase in r/D . Depending on the value of R_s/D , the buckling strength then decreases, reaches a minimum, and then increases rapidly as r/D approaches 0.5 (a hemisphere). For $R_s/D = 1.0$, the minimum

buckling strength is reached at $r/D \approx 0.45$. There may not seem to be a great deal of difference in the shapes of the torisphere at point A in Fig. 2 and the hemisphere at point B. However, the hemisphere is predicted to be 3.25 times as strong as the torisphere corresponding to point A.

Another interesting point about externally pressurized torispheres concerns their optimization insofar as weight and enclosed volume are concerned. This problem was considered recently³ and a simplified form of one of the curves³ is shown in Fig. 3. For each of the two curves shown in Fig. 3, the weights of all the torispheres are the same. However, the torisphere at point A in Fig. 3 has 3.5 times the buckling strength of the torisphere at point C. The ratio of the strengths for points D and E is 8.0. In Fig. 3, the buckling strength p_T and, the enclosed volume V_T have been normalized using a reference hemisphere that has the same weight as the corresponding torispheres.

The preceding predictions are theoretical and they are for perfect hemispheres and torispheres. The shell buckling program used to calculate the buckling/collapse pressures was BOSOR 5.⁴ The tests reported here represent the first experimental verification of these theoretical results.

Scope and Objectives of the Present Work

In order to obtain near-perfect shell models, the torispheres and the hemispheres were machined on a Computer Numeric Controlled (CNC) lathe. Six 0.2-m-diam mild steel models were used to verify the curve in Fig. 2. All had $R_s/D = 1.0$, $D/t = 300$, and the r/D ratios were 0.2, 0.3, 0.4, 0.42, 0.45, and 0.5 (the last being a hemisphere). Two more models were used to verify the two tradeoff solutions shown in Fig. 3 (one corresponding to the maximum buckling strength and one to the minimum).

The aims of the present investigation are the following:

1) To verify, experimentally, the predicted variation of the buckling strength of externally pressurized perfect torispheres as a function of the r/D ratio, as illustrated in Fig. 2. In particular, the behavior in the interval $0.35 < r/D \leq 0.5$ was of interest.

2) To show, as a part of 1), that the buckling strength of a hemispherical shell is very sensitive to changes in its shape. The alternative shapes under consideration are all perfect torispherical shells (i.e., they have no initial radial deviations), but the loss in strength can be considerable.

Received July 31, 1989; revision received Jan. 19, 1990. Copyright © 1990 by the American Institute of Aeronautics and Astronautics, Inc. All rights reserved.

*University Research Fellow, Department of Mechanical Engineering.

†Alexander Elder Professor of Applied Mechanics, Department of Mechanical Engineering.

‡Lecturer, Department of Mechanical Engineering.

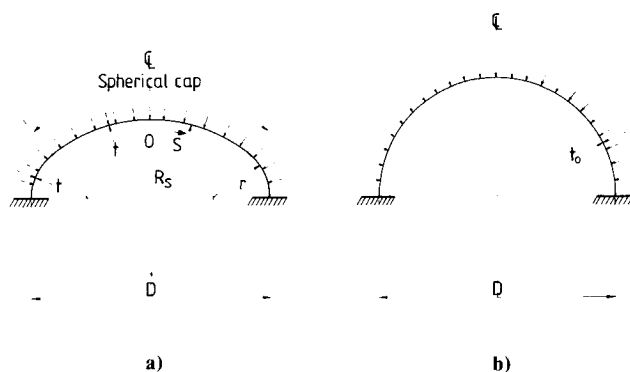


Fig. 1 Geometry of a) torisphere and b) reference hemispheres.

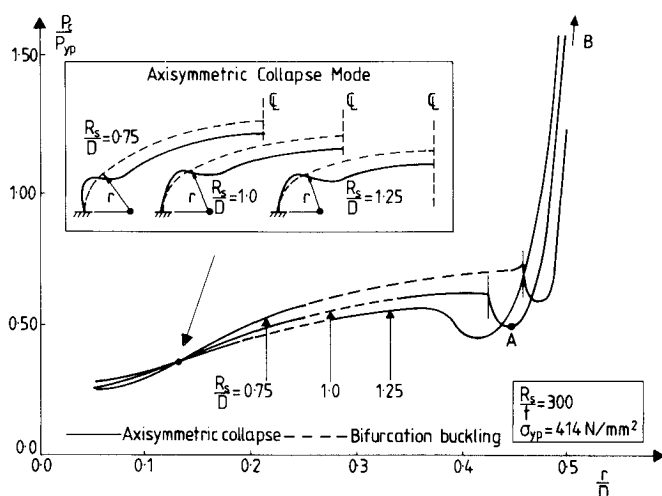


Fig. 2 Dimensionless buckling pressure (bifurcation or collapse) vs knuckle radius/diameter ratio for three torispherical geometries. Note constant shell thickness for each R_s/D ratio.

3) To illustrate experimentally, for a given weight of material in a torisphere, that a near-optimum shape can have a buckling strength that is much greater than that of a poor shape.

4) To show, once again, that the plastic buckling predictions of BOSOR 5 are in good agreement with experimental results on near-perfect shells. This is despite some reservations (which refer to the deformation vs the flow theories of plasticity) noted for internally pressurized torispheres.⁵ The present results are also additional experimental evidence to show that some assertions made⁶ are not correct.

Experimental Details

Manufacture of the Machined Torispherical Domes

The torispheres used in this series of tests were machined from 245-mm-diam billets of mild steel (to BS 4360 Gr.43A). The machine tool used for their manufacture was a Butler 550 lathe that had been retrofitted with a NUM 760T CNC control system.

The sequence of machining operations on these domes was the same as that used for the domes tested recently under internal pressure. That paper⁵ should be consulted for further details.

Thickness Measurement of the Domes

The thicknesses of all the domes were measured at 1 cm intervals meridionally along 8 meridians. The total number of points along each meridian varied between 14 and 18 (depending on the dome). From these measurements, the average thicknesses \bar{t} of the various domes could be determined.

The variations of the actual thickness t in all the domes, relative to their value of \bar{t} , are given in Fig. 4. At any point,

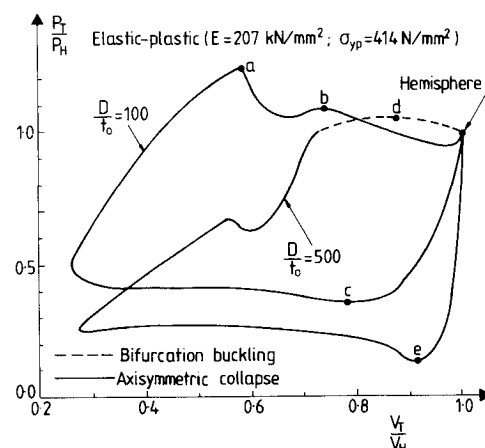


Fig. 3 Envelopes of collapse pressure vs enclosed volume for two reference thicknesses (i.e., $D/t_0 = 100$ and 500). Each curve represents a torisphere of constant weight.

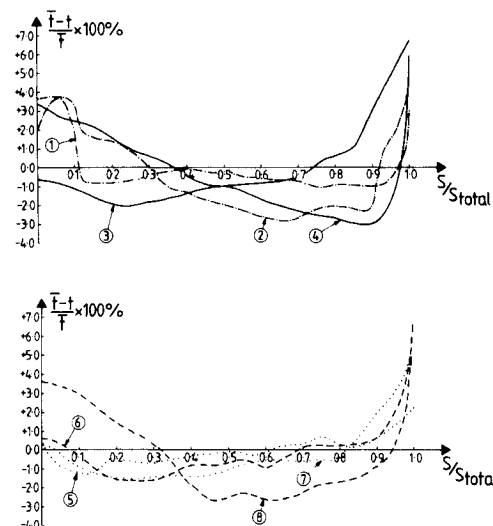


Fig. 4 Variation of mean thickness in torispheres 1-6 vs the arc length s (measured from the apex, toward the clamped boundary).

the value of t in this figure is the average of the thicknesses measured over 8 meridians. (There was not much difference in the thicknesses at the same latitude, when moving from meridian to meridian.) An illustration of the thicknesses actually measured in dome 5 is provided in Table 1. The values of \bar{t} for the various domes are given in column 4 of Table 2.

As may be seen from Fig. 4, the actual thicknesses of the domes differed from their respective values of \bar{t} by less than 4%, for the most part. This value was exceeded only at the edge of the dome, where it rose to +7% in some cases.

Method of Testing the Domes

Each dome was bolted to a steel plate, which acted as an end closure to the dome. A small hole was drilled in the plate, through which water could be introduced (via a bleed pipe) to the interior of the dome before the test. During the test, the amount of water issuing from the bleed pipe served as a measure of the change in volume that was occurring.

The domes plus plates were inserted in a vertical pressure chamber 1 m high \times 0.36 m diam. The chamber pressure was controlled by hand, via a hydraulic pump, and it was measured with a Bell and Howell diaphragm-type pressure transducer and read on a Bruel and Kjaer strain indicator (type 1526). Resolution of the pressure transducer was 1.7×10^{-3} N/mm². The pressure load steps varied from 0.05 to 0.01 of the predicted buckling load—with the latter being used toward the end of an individual test.

In the tests, not much water was expelled from the bleed pipe before failure of the domes occurred. Thus, useful pressure vs change of volume curves were not obtained.

Measurement of Mechanical Properties

Fifteen round and flat tensile specimens were tested to obtain the mechanical properties of the mild steel. Most of the specimens were taken from slices that were perpendicular to the billet axis. (This corresponds to the hoop direction in the models.) However, some tensile specimens taken in the longitudinal direction of the billet were also tested (see Ref. 5 for detailed data).

Typical stress-strain curves obtained on a flat and on a round specimen were illustrated in Fig. 5. As may be seen, there is not much difference between them. This was the case for most of the specimens. The average properties of the mild steel were determined as $\sigma_{yp} = 303.5 \text{ N/mm}^2$, $E = 207.0 \text{ kN/mm}^2$ and $\nu = 0.28$. These values were used in the theoretical calculations for the buckling pressures obtained from BOSOR 5. The steel was assumed to be elastic, perfectly plastic.

Discussion of Results

Buckling Pressures

The experimental and theoretical failure pressures (based on average constant wall thicknesses) of the eight externally pressurized domes are given in Table 2. As may be seen, the agreement between theory and experiment is very good. For some of the models, the test result is slightly higher than the theoretical one (by 5% maximum). However, this small discrepancy can easily be explained by the slight variability one obtains in tests on the mechanical properties of materials.

In addition to using a constant shell wall thickness in the BOSOR 5 program, calculations were carried out using the actual shell thickness, which varied in the meridional direction.

Table 1 Thickness measurements (in mm) at 1 cm intervals along 8 meridians of dome 5

Meridian no.							
1	2	3	4	5	6	7	8
0.667	0.667	0.667	0.667	0.667	0.667	0.667	0.667
0.676	0.674	0.676	0.680	0.678	0.675	0.673	0.676
0.680	0.681	0.675	0.673	0.675	0.680	0.680	0.678
0.674	0.674	0.668	0.663	0.671	0.674	0.674	0.676
0.672	0.675	0.674	0.672	0.674	0.677	0.672	0.677
0.672	0.673	0.673	0.674	0.674	0.674	0.672	0.676
0.672	0.673	0.671	0.671	0.671	0.672	0.672	0.670
0.666	0.673	0.671	0.670	0.671	0.672	0.670	0.671
0.670	0.668	0.670	0.672	0.669	0.669	0.670	0.669
0.670	0.672	0.672	0.672	0.673	0.673	0.671	0.673
0.668	0.670	0.668	0.670	0.667	0.670	0.667	0.668
0.668	0.667	0.666	0.666	0.666	0.669	0.666	0.668
0.663	0.665	0.664	0.663	0.664	0.663	0.665	0.669
0.669	0.671	0.669	0.667	0.668	0.669	0.670	0.670
0.667	0.667	0.666	0.667	0.667	0.670	0.664	0.668
0.661	0.663	0.660	0.664	0.657	0.663	0.663	0.662
0.654	0.661	0.654	0.656	0.649	0.656	0.652	0.654

Table 2 Theoretical and experimental buckling pressures for eight steel machined torispheres subjected to external pressure (dome 6 is hemispherical)

Dome no.	R_s/D	r/D	Average thickness \bar{t} , mm	D/\bar{t}	BOSOR 5 p_c , N/mm ²	Expt. collapse pressure, N/mm ²	$p_{\text{expt}}/p_{\text{BOSOR 5}}$
1	1.0	0.2	0.658	300.9	1.090 (0)	1.103	1.01
2	1.0	0.3	0.653	304.8	1.334 (0)	1.379	1.03
3	1.0	0.4	0.688	292.2	1.511 (0)	1.534	1.02
4	1.0	0.42	0.691	292.3	1.490 (0)	1.569	1.05
5	1.0	0.45	0.669	304.9	1.186 (0)	1.138	0.96
6	Hemisphere		0.684	299.7	3.793 (17)	3.845	1.01
7	0.55	0.30	0.775	258.1	4.104 (12)	4.276	1.04
8	1.25	0.425	0.672	302.1	0.786 (0)	0.819	1.04

This meant that eight BOSOR 5 calculations were made for each dome (see Table 1). It was found that the inclusion of the small variations in meridional thickness had a very small effect on the buckling strength. For example, there was less than 1% scatter in the theoretical buckling pressures when the thicknesses given in Table 1 were used in the calculations.

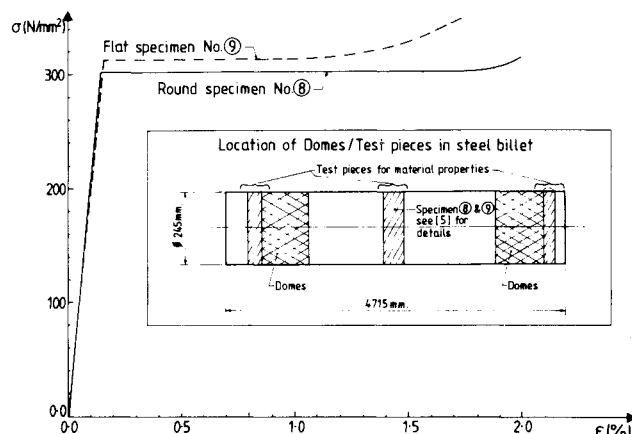


Fig. 5 Typical uniaxial stress-strain curves for flat and round specimens. (Their locations in the steel billet and the regions from which torispheres 1-8 were cut are shown in the insert.)

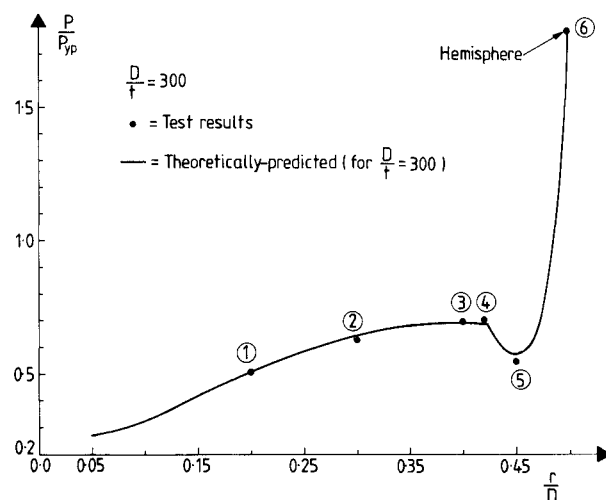


Fig. 6 Six experimental results vs the numerically predicted collapse curve (for $R_s/D = 1$, $D/t = 300$, and $0.05 \leq r/D \leq 0.5$).

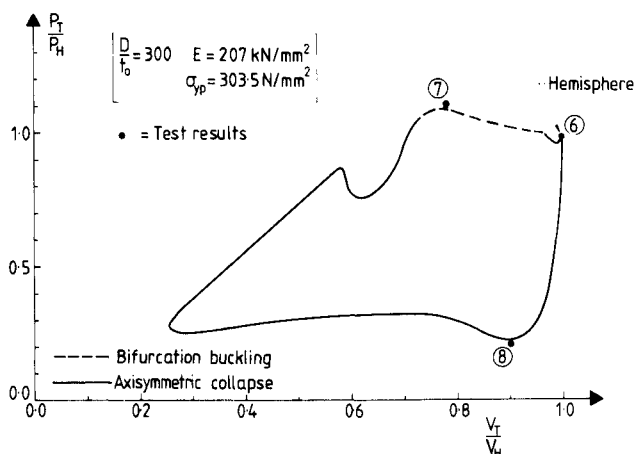


Fig. 7 Stability contour (collapse pressure vs enclosed volume) for a torisphere. Experimental points represent two different tradeoff solutions (domes 7 and 8).

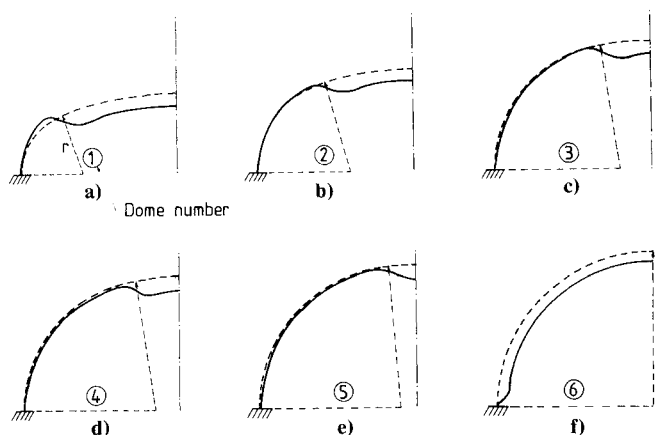


Fig. 8 Deformed shapes of tradeoff solutions (i.e., domes 7 and 8, Figs. 8a and 8b) together with weight/material equivalent hemispheres (Fig. 8c). Bifurcation mode for domes 7 and 6 in Figs. 8d and 8f. Comparison of initial shapes in Fig. 8e.

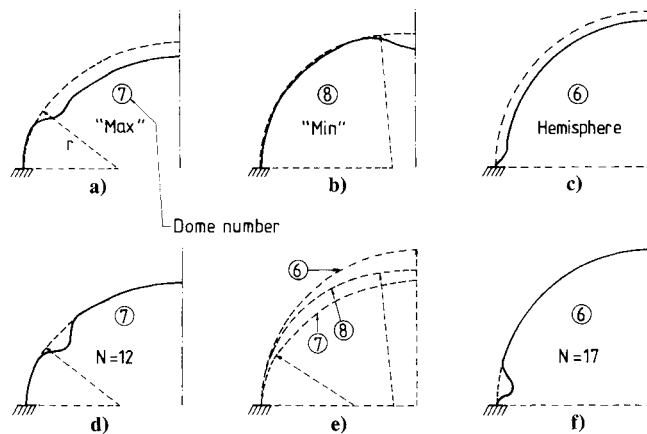


Fig. 9 Deformed shape prior to buckling for domes 1-6 (see also Fig. 6 for their buckling behavior).

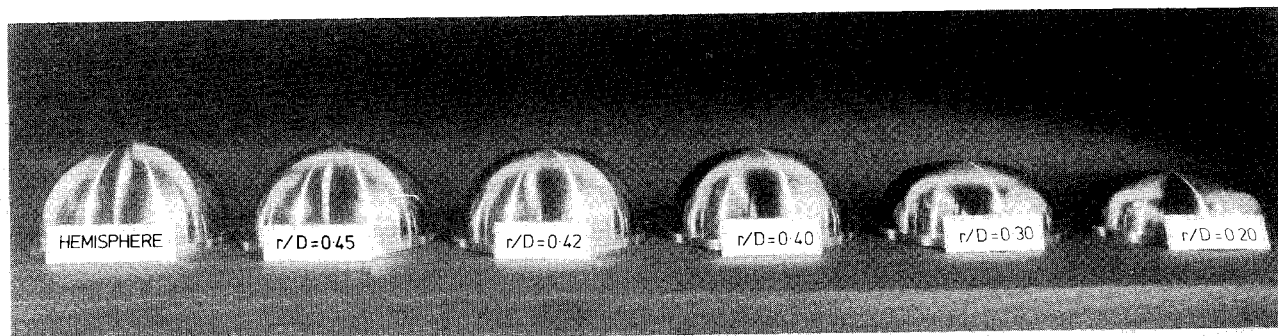


Fig. 10 Six machined domes before testing. From left to right: $r/D = 0.5$ (hemisphere), $r/D = 0.45$, 0.42 , 0.40 , 0.30 , and 0.2 . All domes were of constant thickness.

Insofar as the buckling strength of the perfect torispherical domes vs the r/D ratio is concerned, the results in Fig. 6 constitute a very good experimental verification of the theoretical predictions. The test results for domes 3-6 are particularly interesting, as they show the unexpected dip in the buckling strength around $r/D = 0.45$. The shapes of domes 5 and 6 are not that different, yet their experimental strengths are in the ratio 1:3.34.

It is, of course, well known that the buckling resistance of hemispherical shells is very susceptible to the presence of initial radial deviations. However, the theoretical collapse pressures shown in Fig. 6 are for perfect shells. The decrease in the buckling strength when going from dome 6 to dome 5 is due to the r/D changing from 0.5 to 0.45 (with all other factors remaining the same). (See also the later subsection "Some Additional Comments.")

With regard to the search for an optimum torispherical shape, the two test results in Fig. 7 confirm the maximum and minimum values of the two curves in Fig. 3. Even though one of the R_s/D ratios is 0.55 (dome 7) and the other is 1.25 (dome 8), the difference in the two overall shapes is not that great—see Fig. 8e. However, the ratio of the two experimental failure pressures is 5.22:1.

For domes 7 and 8, the R_s/t ratios are 142 and 377.5, respectively. If elastic buckling of the spherical portion of the torisphere controlled the failure mode, i.e., $p_{cr} \propto (t/R_s)^2$, then one would expect the ratio of the buckling strengths of the two domes to be $(377.5/142)^2 = 7.07$. This point was made by one of the referees of the paper. However, for domes 7 and 8, failure occurred by plastic buckling or collapse. The ratio of the buckling strengths given by elastic theory is too high by about 35%.

It should be noted that, in this paper, the torispheres under discussion have been perfect (the experimental models were "near perfect"). As most domes in practice have geometric

imperfections in them, it is of interest to know how the results in this paper change for imperfect shells. The authors hope to answer this question in the near future.

The present dome 8 could be considered as a hemispherical shell with an increased-radius "flat" spot at the apex (with the radius of the imperfection being greater than the radius of the hemisphere). Such imperfections have been considered before,⁷⁻⁹ both in the elastic and the plastic buckling regions. In those references, there was a discontinuity in slope at the junction of the hemispherical shell with the flat spot, but this is not present in dome 8 (which is a perfect torispherical shell). However, the effect of the slope discontinuity on the buckling pressure is not expected to be large.

Failure Mode

The numbers of circumferential waves n at buckling predicted by BOSOR 5 for domes 1 to 8 are given in parentheses in column 5 of Table 2. As may be seen, the theoretical failure mode is axisymmetric collapse (i.e., $n = 0$) for domes 1-5 and 8, and is bifurcation buckling for domes 6 and 7. Sketches of the theoretical shapes of the deformed domes just prior to failure are given in Figs. 8a and 8b and Figs. 9a-9f. The two theoretical buckling modes (for domes 6 and 7) are shown in Figs. 8d and 8f.

It should be noted that, on Fig. 2, the dome with $r/D = 0.3$, $R_s/D = 1.0$ is predicted to fail by bifurcation buckling, whereas n for dome 2 in Table 2 is given as $n = 0$. The different predictions are due to different values of σ_{yp} being used in the calculations.

The actual experimental failure modes are shown in Figs. 10-12. The domes that were predicted to fail in an axisymmetric manner ($n = 0$ in Table 2) did so in the tests. The predicted failure mode for the clamped hemisphere was edge buckling ($n = 17$), but the experimental result was the single

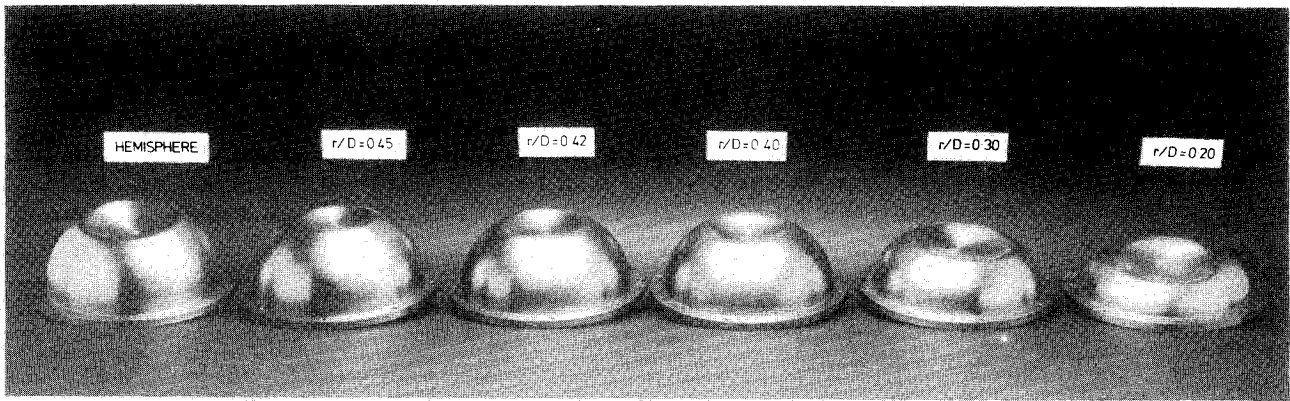


Fig. 11 Domes 6, 5, 4, 3, 2, and 1 (from left to right) after testing.

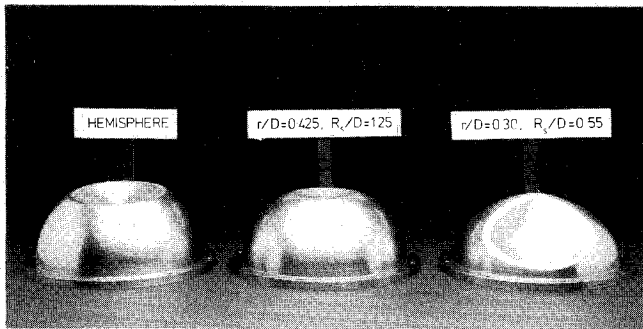


Fig. 12 Domes 6, 8, and 7 after testing.

buckle shown in Figs. 11 and 12. For dome 7, also, the test result was a single buckle instead of the predicted 12 waves. However, as is known, it is very difficult to obtain the complete bifurcation buckling modes for shells, particularly when they fail by plastic buckling. Figures 11 and 12 also show postbuckled shapes. It is possible that the bifurcation modes could be obtained by inserting a mandrel inside the shell, as was done in Ref. 10.

Some Additional Comments

For torispherical shells with large r/D ratios (in the range 0.42–0.5, say), the failure region moves from the vicinity of the knuckle/spherical cap junction to the apex. The reduction in buckling strength that occurs (relative to that of a hemisphere) depends on the size of the spherical cap. As has been noted in Ref. 11, the steep drop in the buckling strength that occurs in Fig. 6 when going from $r/D = 0.5$ to 0.45 can be ascribed to the deviation from sphericity of the $r/D = 0.45$ torispherical shell. This point was also noted by one of the referees.

However, the increase in strength in going from $r/D = 0.45$ to 0.40 is a little harder to explain. It is hoped it will be possible to publish a detailed numerical/experimental analysis of the whole $0.35 < r/D < 0.5$ region in the near future.

Conclusions

The present series of tests, on externally pressurized, near-perfect machined torispherical and hemispherical shells having $R_s/t \approx 300$ and made from mild steel has shown that:

- 1) The predicted and unexpected dip in the collapse pressure vs r/D curve (see Fig. 6) does actually occur.
- 2) The predicted rapid loss in the buckling resistance of a hemispherical shell (due to changing the r/D ratio from 0.5 to, say, 0.45) also occurs. The ratio of the two test results was 3.34:1.

3) The choice of an optimum shape of torisphere (while keeping the weight the same) can result in a fivefold increase in the buckling resistance compared to that of a poor shape.

4) The predictions of the BOSOR 5 shell buckling program agreed very well with the test results. By implication, this supports the validity of the numerical results given,¹² which were based on BOSOR 5.

The preceding conclusions apply to near-perfect shells. Initial geometric imperfections will change the various buckling pressures. The effects of initial imperfections on the overall conclusions of this paper will be reported in a future paper.

References

- ¹Blachut, J., and Galletly, G. D., "Clamped Torispherical Shells Under External Pressure—Some New Results," *Journal of Strain Analysis*, Vol. 23, No. 1, 1988, pp. 9–24.
- ²Blachut, J., and Galletly, G. D., "Externally-Pressurized Torispheres—Plastic Buckling and Collapse," *Buckling of Structures—Theory and Experiment*, edited by I. Elishakoff, J. Arbocz, D. C. Babcock, Jr., and A. Libai, Elsevier, Amsterdam, Holland, 1988, pp. 29–45.
- ³Blachut, J., "Multiobjective Optimization of Externally-Pressurized Torispheres under Buckling Constraints," *Computer Aided Optimum Design of Structures—Applications*, edited by C. A. Brebbia and S. Hernandez, Springer-Verlag, Berlin, 1989, pp. 145–155.
- ⁴Bushnell, D., "BOSOR 5—Program for Buckling of Elastic-Plastic Complex Shells of Revolution Including Large Deflections and Creep," *Computers and Structures*, Vol. 6, No. 3, 1976, pp. 221–239.
- ⁵Galletly, G. D., Blachut, J., and Moreton, D. N., "Internally-Pressurized Machined Domed Ends—A Comparison of the Plastic Buckling Predictions of Deformation and Flow Theories," *Proceedings of the Institution of Mechanical Engineers*, London, England, No. C3, Vol. 204, 1990, pp. 169–186.
- ⁶Uddin, M. W., "Buckling of General Spherical Shells Under External Pressure," *International Journal of Mechanical Sciences*, Vol. 29, No. 7, 1987, pp. 469–481.
- ⁷Bushnell, D., "Nonlinear Axisymmetric Behavior of Shells of Revolution," *AIAA Journal*, Vol. 5, No. 3, 1967, pp. 432–439.
- ⁸Koga, T., and Hoff, N. J., "The Axisymmetric Buckling of Initially-Imperfect Complete Spherical Shells," *International Journal of Solids and Structures*, Vol. 5, No. 7, 1969, pp. 679–697.
- ⁹Galletly, G. D., Blachut, J., and Kruszelecki, J., "Plastic Buckling of Imperfect Hemispherical Shells Subjected to External Pressure," *Proceedings of the Institution of Mechanical Engineers*, London, England, Vol. 201, No. C3, 1987, pp. 153–170.
- ¹⁰Carlson, R. L., Sendlebeck, R. L., and Hoff, N. J., "Experimental Studies of the Buckling of Complete Spherical Shells," *Experimental Mechanics*, Vol. 7, July 1967, pp. 281–288.
- ¹¹Galletly, G. D., and Blachut, J., "On the Buckling Strength of Steel and CFRP Dome Closures," *Proceedings of the Undersea Defence Technology '90 Conference*, Microwave Exhibitions and Publishers, London, England, Feb. 1990.
- ¹²Blachut, J., "Search for Optimal Torispherical End Closures Under Buckling Constraints," *International Journal of Mechanical Sciences*, Vol. 31, No. 8, 1989, pp. 623–633.